Thesis（Dissertation）

Laeverin/aminopeptidase Q induces indoleamine 2,3-dioxygenase-1 in human monocytes

The Graduate School of Medical Sciences

Kanazawa University

(Supervisor: Prof. Hiroshi Fujiwara *Research Field: Obstetrics & Gynecology)

Student ID : 2028062017

Name : Takuma Suzuki

Table of Contents

Abstract

Human extravillous trophoblast (EVT) invades the maternal endometrium and reconstructs uterine spiral arteries cooperatively with maternal immune cells. Although EVT has allogeneic paternal antigens, the maternal immune system does not reject it. Here, we found that laeverin (LVRN), an EVT-specific cell surface peptidase, interacts with monocytes to produce indoleamine 2,3-dioxygenase-1 (IDO1). LVRN-transfected Swan71 cells, a cytotrophoblast-derived cell line, increased IDO1 expression in PBMC under cell-to-cell interacting conditions. Soluble recombinant LVRN (r-LVRN) interacted with CD14-positive monocytes and induces their IDO1 expression without the intervention of other immune cell populations. LVRN-induced IDO1 production was promoted in PMA-activated monocyte-like THP-1 cells. Furthermore, r-LVRN decreased the tryptophan level and increased the kynurenine/tryptophan ratio in the culture media of the PMA-treated THP-1 cells. These findings suggest that LVRN is one of the key molecules that mediate the interaction between EVT and monocytes/macrophages and creates an immunosuppressive environment at the maternal-fetal interface in the uterus.

Introduction

Human extravillous trophoblast (EVT) is derived from cytotrophoblast. EVT invades the maternal endometrium and reconstructs maternal spiral arteries [1]. This enables to supply an adequate amount of maternal blood into the intervillous spaces [2]. If this remodeling in the early stage of pregnancy is incomplete, it later leads to placental dysfunction and preeclampsia. During the process of invasion, EVT was reported to directly interact with various kinds of maternal cells such as decidual uterine natural killer (NK) cells and macrophages in the endometrium and cooperatively remodel spiral artery with these maternal immune cells in a spatiotemporally regulated manner [3-5].

Although EVT has allogeneic paternal antigens, it is not rejected by the maternal immune system. Recently, as an embryonic signal, human chorionic gonadotropin (hCG), which is specifically secreted from intraplacental syncytiotrophoblast, was reported to be involved in the acquisition of immunotolerance by controlling regulatory T cell functions [6-8]. In contrast to syncytiotrophoblast, the production of hCG by EVT is limited. EVT is abundantly resident throughout the uterus during pregnancy and has an immune-activating ability to induce maternal-fetal tolerance [9]. HLA-G is specifically expressed on EVT and interacts with various receptors on maternal immune cells. It can trigger either inhibitory or stimulatory signals in decidual T cells, NK cells, macrophages, or dendritic cells, leading to immune tolerance and vascular remodeling in placental development [10,11]. Recently, the role of HLA-E and HLA-F, which are also HLA class Ib molecules, in the induction of immune tolerance has received much attention [12,13]. However, the cellular interactions mediated through these HLA molecules cannot fully explain the mechanisms by which EVT acquires immune tolerance during human placentation.

Previously, we identified an EVT-specific cell surface peptidase, laeverin/aminopeptidase Q, which belongs to the M1 peptidase family [14,15]. Laeverin (LVRN) was specifically expressed on EVT in the human placentas throughout pregnancy. In primary villous explant cultures, LVRN expression was induced on the cell surface of the outgrowing EVT and the cultured EVT secreted a soluble form of LVRN [16]. Recombinant soluble form of LVRN (r-LVRN) promoted EVT invasion in vitro, whereas gene reduction of LVRN attenuated EVT invasion, indicating that LVRN regulates EVT invasion [16]. Since the expression of LVRN is specifically limited to

the placenta, especially in EVT, LVRN is speculated to play a specific role in the regulation of the maternal immune response against EVT. However, there is little information about its immunological functions.

Based on this background, to investigate the roles of LVRN in the acquisition of immunotolerance in EVT, we examine the effects of LVRN on immune cell function using PBMC, a monocytic cell line, THP-1 [17], and LVRN-transfected immortalized EVT cell line, Swan71 [18]. Since indoleamine 2,3-dioxygenase-1 (IDO1), which has an immunosuppressive function by limiting T-cell function [19,20], was reported to play important roles in the regulation of an immunotolerant environment during pregnancy [21], we focused on the effects of LVRN on the production IDO1 in this study.

Material and Methods

Experimental model and subject details

Isolation of human peripheral blood mononuclear cells (PBMC)

Blood was collected from healthy Japanese male and female (male, n=7, mean age=30.7(28-35); female, n=10, mean age=29.9 (26-37)) volunteers under heparinized conditions. Collecting the blood samples was approved by the Medical Ethics Committee of Kanazawa University (approval number: 2019-12(3152)), and written informed consent was received from participants. PBMC were isolated using Ficoll-Paque^{TM} PLUS (Cytiva, density 1.077±0.001g/mL). Isolated PBMC were frozen in CELLBANKER1 at -80°C until use. The day before use, PBMC were dissolved and cultured in RPMI supplemented with 10% Heat Inactivated FBS (Sigma-Aldrich), 100 g/mL streptomycin, and 100 IU/mL penicillin. To collect CD14-positive monocytes, PBMCs were reacted with CD14 MicroBeads (Miltenyi Biotec). Then, CD14 cells were isolated with the Possel program of autoMACS® Pro Separator (Miltenyi Biotec).

Human placenta tissue

Human term placental tissues were obtained from normal Japanese pregnancies (n=5). Informed consent for the use of these tissues in this study was obtained from all donors. Analysis of these samples was approved by the Medical Ethical Committee of Kanazawa University (approval number: 2015-009 (388)).

Cell lines and cell culture

The human acute monocytic leukemia cell line THP-1 (RRID: CVCL_0006) was purchased from ATCC. To activate THP-1 cells, we added Phorbol12-myristate13-acetate (PMA, Sigma-Aldrich) and cultured them for 48h. Swan71 (RRID: CVCL_D855) was gifted by Prof. Mor G, which is human telomerase reverse transcriptase-transfected immortalized first-trimester trophoblast cell line [18]. Both cell lines were authenticated by STR profiling. To establish LVRN-transfected Swan71 cells (Swan71_LVRN), hLVRN-His cDNA was inserted into pTargeT vector (Promega). Then, r-LVRN-His/pTargeT (500 ng) was cleaved and linearized with Psp1406I and transfected into Swan71 cells using FuGeneHD (Promega). After 48 hours of gene transfer, a stable expression strain was established and isolated using a medium containing 500 μg/mL G418. For controls, the non-inserted pTargeT vector was transfected into Swan71

cells (Swan71_NEO). Cell lines were maintained at 37 °C under 5% CO_2 in RPMI (Nacalai Tesque, Kyoto, Japan) supplemented with 10% FBS (Sigma-Aldrich), 100 g/mL streptomycin, and 100 IU/mL penicillin. Mycoplasma infections were detected regularly, and all experiments were performed under mycoplasma-free conditions.

Method details

Co-culture of PBMC with LVRN-transfected Swan71 cells

For the co-culture with direct contact, Swan71_LVRN and Swan71_NEO cells pre-treated with 2 μg/mL of mitomycin for 4 hours were cultured at a concentration of $1.5x10^5$cells/well with RPMI 1mL/well using 12-well plates. After cell adhesion was confirmed, 1 mL of PBMC prepared in RPMI at a concentration of $1.5x10^5$ cells was replaced with the culture medium of Swan71_LVRN or Swan71_NEO cells and incubated at 37°C for 24 hours. The culture plates were agitated with a shaker for 10 minutes. The floating cells were collected and filtered twice with a 35-μm pore cell strainer. In addition, CD45 MicroBeads (Miltenyi Biotec) were reacted, and CD45-positive cells were selectively collected by the Possel program of autoMACS® Pro Separator (Miltenyi Biotec). For the co-culture with indirect contact, mitomycin-treated Swan71_LVRN and Swan71_NEO cells were cultured in a 6-well plate for adherent cells at a concentration of 3.0×10^5 cells/well in RPMI (3 mL/well), respectively. After confirming cell adhesion, PBMC (1.0×10^5 cells/well) in a 0.4 μm transwell (Greiner Bio-One®) was placed on the plate and incubated at 37°C for 24 hours and was recovered.

RT-PCR and quantitative real-time PCR analysis

RT-qPCR was performed as described previously [31]. Total RNA was extracted from PBMC and cell lines using the RNeasy mini kit (Qiagen, Hilden, Germany) according to the manufacturer's instructions. This RNA was reverse transcribed into cDNA using PrimeScript™ RT-PCR Kit (Takara Bio Inc., Shiga, Japan). β-actin (ACTB) was used as a control. cDNA was amplified using the specific primers for IDO1 (Fd 5'-GGCACACGCTATGGAAAACT-3'; Rs 5'-CGGACATCTCCATGACCTTT-3:) and ACTB (Fd 5'-TGGCACCCAGCACAATGAA-3'; Rs 5'-CTAAGTCATAGTCCGCCTAGAAGCA-3'). PCR was performed using SYBR Premix Ex Taq (Takara) following the PCR protocol. The cycling conditions were initial denaturation at 95°C for 30 seconds, denaturation at 95°C for 5 seconds, and annealing/extension reaction at 60°C for 30 seconds for 40-45 cycles. Quantitative real-time PCR (qPCR) analysis was performed on an AriaMX Real-Time PCRsSystem (Agilent Stratagene, La Jolla, Calif., USA) according to the manufacturer's instructions. Mean ± SEM of 3-5 independent experiments is shown.

Absorption of r-LVRN by anti-His-tag antibody-conjugated beads

r-LVRN and E416Q mutated r-LVRN protein, which was lost with aminopeptidase enzymic activity were prepared as previously reported [15,29]. Since r-LVRN contains His-tag, we used anti-His-tag antibody-conjugated magnetic beads to absorb r-LVRN molecules. Briefly, both 1 μL of Bc MagTM His-Ni magnetic Beads (Cat#MHN-102, LOT: 0119) and 4.5 μg of r-LVRN were added to 400 μL of PBS and stirred at 4°C. After 30 minutes, a magnet (6-Tube Magnetic Separation Rack, Cell Signaling) was used to recover the beads and the r-LVRN that had reacted with the beads. The supernatant was used as an r-LVRN-absorbed agent.

Immunofluorescent staining of cells

Fluorescent labeling of r-LVRN was carried out according to the manual using AnaTag HiLyte Fluor 488 Microscale Protein Labeling Kit (AnaSpec Inc, Fremont, CA, USA). To investigate the cell binding of r-LVRN, cultured THP-1 cells or PBMCs were cultured with HiLyte Fluor 488-labeled r-LVRN (1.5 μg/mL). After incubation, they were fixed with 4% paraformaldehyde and observed under a fluorescence microscope. For LVRN staining, Swan71 cells were fixed with 4% paraformaldehyde for 10 minutes, incubated with a mouse anti-human LVRN monoclonal antibody (1 μg/mL, clone 5-23) [14], and then reacted with Alexa Fluor 488 goat anti-mouse IgG(H+L) (1:500, Thermo Fisher Scientific Cat# A-11001, RRID: AB_2534069). After washing, they were embedded, observed under a fluorescence microscope (Olympus BX50 microscope), and photographed with a camera (DP72 Olympus digital camera, Tokyo, Japan).

Immunofluorescent staining of placenta

For immunofluorescence staining of placenta tissue, we fixed them using two different ways. For staining LVRN, CD68, and CD163, we mounted the fresh tissues in OCT, sliced them into 8 μm thickness, fixed them in -20° C acetone for 5 min, and immediately dried them out by cold wind. They were blocked by 10%FBS/PBS. We sliced them into 8 μm thickness and used 0.1% triton in 10%FBS/PBS for blocking. After blocking, we incubated with primary antibodies against LVRN (1 μg/mL), CD68 (1:400, Cell Signaling Technology, Cat #76437, RRID:AB_2799882), and CD163 (1:200, Proteintech, Cat#16646-1-AP, RRID:AB_2756528) for 1 day at 4° C. After washing in PBS, we reacted with secondary antibodies: Alexa Fluor 488 goat anti-mouse IgG(H+L) and Alexa Fluor 555 goat anti-rabbit IgG(H+L) (Invitrogen, Cat#A32732, RRID: AB_2633281), and Hoechst for 2 h at room temperature. After washing them, we mounted under-cover slips with Mowiol, observed them under a fluorescence microscope, and photographed them with a camera.

Flow cytometrical analyses

Swan71 cells were incubated with FITC-labeled anti-LVRN antibody (1μg/mL, clone 5-23) or control mAb for 30 minutes at 4°C. Cell surface labeling was analyzed by a BD FACS Aria™ Fusion cell sorter. To evaluate the binding ability of immune cells to r-LVRN, PBMC were incubated with 1.5 μg/mL of HiLyte Fluor 488-labeled r-LVRN for 4 or 24 hours and fixed with 4% paraformaldehyde for 10 minutes. Then, the fluorescence intensities of the monocyte and lymphocyte fractions in PBMC were analyzed using a BD FACS Aria™ Fusion cell sorter. To evaluate which immune cells interact with r-LVRN, PBMC were incubated with 1.5 μg/mL of HiLyte Fluor 488-labeled r-LVRN for 24h and we fixed with 4% paraformaldehyde. Then, we react them with a mouse BV421-conjugated anti-human CD14 monoclonal antibody (4 μL/test, Thermo Fisher Scientific Cat# 17-9477-42, RRID: AB 2716946), mouse BV421-conjugated anti-human CD3 (4 μL/test, BD Biosciences Cat# 562426, RRID: AB_11152082) and BV421-conjugated anti-human CD19 (4 μL/test, BD Biosciences Cat# 562440, RRID: AB_11153299) after blocking with BD PharmingenTM Human BD Fc blockTM (Cat#564220, LOT: 9049805). After 1h, these signals were detected by a BD FACS Aria™ Fusion cell sorter. IDO1 expression in r-LVRN-treated PBMC was also analyzed by flow cytometry. PBMC were cultured with 1.5 and 7.5 μg/mL of r-LVRN for 24 hours. After blocking with BD

PharmingenTM Human BD Fc blockTM, a mouse BV421-conjugated anti-human CD14 monoclonal antibody was allowed to act at 4°C for 1 hour. After washing, PBMC were fixed with 1% paraformaldehyde, permeabilized with 0.1% triton/PBS, and reacted with a mouse APC-conjugated anti-human IDO antibody (5 μL/test, Thermo Fisher Scientific Cat# 17-9477-42, RRID: AB_2716946) at 4°C for 1 hour. Fluorescence was detected using a BD FACS Aria^{TM} Fusion cell sorter.

Western blot analysis

Western blot analysis was performed as described previously [32]. Protein lysates were extracted with RIPA Buffer (Cell Signaling Technology Inc., Danvers, MA, USA), and were electrophoresed on a 10% SDS-PAGE gel and then transferred to a nitrocellulose membrane. The transferred membranes were incubated with primary antibody against IDO (1:1000, Cell Signaling Technology Cat# 86630, RRID: AB_2636818) or Actin (1:5,000, Santa Cruz Biotechnology Cat# sc-1615, RRID: AB_630835) overnight at 4oC. A secondary horse-radish peroxidase (HRP) conjugated antibody was applied for 1 hour at room temperature. The blots were visualized with an enhanced chemiluminescence system using ECL^{TM} Western Blotting Detection Reagents (GE Healthcare, Buckinghamshire).

High-performance liquid chromatography-mass spectrometry (HPLC-MS)

The levels of tryptophan and kynurenine in the culture medium were quantified by High-Performance Liquid Chromatography and High-Resolution Mass Spectrometry and Tandem Mass Spectrometry (HPLC-MS/MS). To evaluate the difference between vehicle and r-LVRN treatment, the PMA-activated THP-1 cells were treated with 1.5 and 7.5 μg/mL of r-LVRN for 48 hours. Then metabolite levels in the culture medium were measured by HPLC-MS at Institute for Gene Research, Kanazawa University as previously described [33]. The kynurenine/tryptophan ratio was calculated to evaluate the activity of the IDO1.

Statistical analysis

All statistical analyses were performed using R software [30]. One-way ANOVA (Analysis of variance) with post hoc t-test with Bonferroni correction or Kruskal-Wallis test with post hoc Wilcoxon signed-rank test with Bonferroni correction was performed to compare the data between each treatment group. Welch two-sample t-test or Wilcoxon signed-rank test was performed to compare the data between the two experimental groups. Detailed descriptions of statistical analysis and the sample size are described in each figure legend. A P-value of < 0.05 was considered significant.

Results

LVRN-transfected Swan71 cells promoted IDO1 expression in PBMC

To investigate the immunological roles of LVRN that is expressed on the cell surface of EVT, we produced LVRN-transfected Swan71 cells (Swan71_LVRN) and mock-transfected Swan71 cells (Swan71_NEO). Immunofluorescence staining showed protein expression of LVRN in

Swan71_LVRN (Fig. 1A). The cell surface expression of LVRN in Swan71_LVRN was also confirmed by the flow cytometric analysis (Fig. 1B). Under direct contact conditions, the mRNA expressions of IDO1 in PBMC were significantly enhanced by co-culture with LVRN-transfected Swan71 cells than those with mock-transfected Swan71 cells (Fig. 1C). In contrast, under indirect contact conditions using trans-wells, the co-culture with LVRN-transfected Swan71 cells did not increase IDO1 expression in PBMC (Fig. 1C). These results indicate that direct interaction of LVRN with immune cells is necessary to induce IDO1 production in PBMC and that other soluble factors secreted from LVRN-transfected Swan71 cells are not involved in the LVRN-dependent increase in IDO1 expression.

Soluble LVRN promoted IDO1 expression in PBMC

To investigate the specific effects of LVRN on IDO1 expression in PBMC, we then examined the effects of r-LVRN, a soluble form of LVRN [15,16], on the IDO1 gene expression in PBMCs. r-LVRN treatment significantly upregulated IDO1 gene expression in a dose-dependent manner (Fig. 2A) in PBMCs compared to vehicle controls. We also treated with E416Q mutated r-LVRN protein, which was lost with aminopeptidase enzymic activity [15]. E416Q r-LVRN treatment increased IDO1 expression similar to the wild-type r-LVRN (Fig. 2B), indicating that the effect of r-LVRN is independent of enzyme activity. Since r-LVRN was produced by the baculovirus expression vector system [15], the virus-derived contamination might have affected the results. To exclude the adverse effects of contamination, we conducted the absorption experiment. Since r-LVRN contains His-tag, we used anti-His-tag antibody-conjugated magnetic beads to absorb r-LVRN molecules. When we removed the r-LVRN by beads, the r-LVRN effect disappeared (Fig. 2C), indicating that r-LVRN itself increased IDO1 gene expression.

r-LVRN interacted with CD14-positive monocytes

Next, to explore the target cells of r-LVRN, we treated PBMCs with fluorescent-labeled r-LVRN. Flow cytometric analysis showed that r-LVRN was bound to the monocyte-rich fraction (Fig. 3A), but not to the lymphocyte-rich fraction (Fig. 3B). The r-LVRN-positive population increased during the 24-hour culture. In addition, we demonstrated that r-LVRN was bound to 98% of CD14-positive cells (Fig. 3C), 0.4% of CD3-positive cells (Fig. 3D), and 13 % of CD19-positive cells (Fig. 3E). We also confirmed the cell surface binding of r-LVRN to CD14-positive cells by immunocytochemistry (Fig. 3F).

r-LVRN induced IDO1 expression in CD14-positive monocytes

To evaluate the direct effects of r-LVRN on monocytes, CD14-positive cells were isolated from PBMC. r-LVRN treatment significantly promoted IDO1 mRNA levels in CD14-positive monocytes (Fig. 4A). Then, to validate that r-LVRN binds to CD14-positive monocyte and induces IDO1 protein expression, we treated PBMCs with r-LVRN and stained them with anti-CD14 and anti-IDO1 antibodies. The protein expression of IDO1 was induced in CD14-positive cells in a dose-dependent manner (Figs. 4B-D).

r-LVRN induced IDO1 expression in PMA-stimulated THP-1 cells

Since the reactivity to r-LVRN in CD14-positive monocytes increased during the 24-hour culture, we then employed a monocyte-lineage cell line, THP-1 cells, to assess whether

activated monocytes enhance the reactivity to r-LVRN or not. The r-LVRN treatment showed little effect on IDO1 gene induction in non-activated THP-1 cells (Fig. 5A). In contrast, IDO1 gene expression was slightly induced in the Propidium monoazide (PMA)-activated THP-1 cells and r-LVRN treatment further enhanced IDO1 expression (Fig. 5A). Western blot analysis validated the dose-dependent increase in IDO1 protein by r-LVRN treatment (Fig. 5B). r-LVRN increased IDO1 gene expression after 8 h of treatment in PMA-activated THP-1 cells (Fig. 5C). Western blot analysis showed that IDO1 protein expression reached plateau levels within 12 hours after r-LVRN treatment (Fig. 5D).

r-LVRN decreased the tryptophan level and increased the kynurenine/tryptophan ratio in PMA- activated THP-1 cells

The effects of r-LVRN-induced IDO1 production on the conversion of tryptophan into kynurenine were evaluated by high-performance liquid chromatography-mass spectrometry (HPLC-MS). HPLC-MS showed that r-LVRN treatment decreased the tryptophan level (Fig. 6A) and increased the ratio of kynurenine/tryptophan (Fig. 6B) in the culture media derived from PMA-activated THP-1 cells compared to the r-LVRN-non-treated controls.

Macrophages are closely associated with LVRN-positive EVT at the maternal-fetal interface of the term placenta

We performed double immunohistochemical staining of macrophage markers and LVRN in the term placenta and observed that CD68- and CD163-positive macrophages contact LVRN-positive EVT at the maternal-fetal interface of the placental bed and fetal membrane (Fig. 7).

Discussion

IDO1 is a rate-limiting enzyme that catalyzes tryptophan to convert into kynurenine. Local depletion of tryptophan induces an immunosuppressive environment that inhibits the proliferation of effector T lymphocytes [22,23] and the increase in kynurenine promotes T cell differentiation towards regulatory T lymphocytes [24]. First, this study showed the possibility that cell surface LVRN elicits IDO1 production in immune cells by the cell-to-cell interaction using the co-culture system of LVRN-transfected Swan71 cells and PBMC, suggesting the involvement of LVRN in creating an immunosuppressive environment around EVT.

Although the significant differences in induction of IDO1 expression between LVRN- and mock-transfected Swan71 cells suggest specific effects of LVRN, the possible involvement of other cell surface molecules, which are induced by LVRN-gene transfection, cannot be excluded. To answer this question, we investigated the effects of a soluble form of LVRN, r-LVRN, and observed similar findings that IDO1 expression was induced in the r-LVRN-stimulated PBMC. Furthermore, we confirmed that the effects of r-LVRN disappeared when it was absorbed by anti-His-tag antibody-conjugated magnetic beads, indicating that r-LVRN itself, but not contamination, increased IDO1 gene expression. From these findings, we concluded that LVRN specifically induces IDO1 expression in PBMC. It is also noted that peptidase enzyme activity is not necessary for the inducing effect of r-LVRN on IDO1

expression. In addition, LVRN has glycosylation and the molecular mass of LVRN produced by the human-derived Swan71 cells is about 160kD, while that of r-LVRN produced by baculovirus is 120kD because it lacks an N-terminal site (64 amino acid sequences) responding to the membrane binding domain and has a very small size of glycosylation [15]. Therefore, the similar effects between LVRN expressed on Swan71 and r-LVRN suggest that the majority of glycosylation structures are not involved in the induction of IDO1 production.

The circulating monocytes and decidual macrophages were reported to play a critical role in regulating the local immune environment at the maternal-fetal interface [25]. The present study showed that r-LVRN interacts with the cell surface of CD14-positive monocytes, indicating that monocytes are target cells of LVRN. This suggests the presence of LVRN receptors on CD14- positive monocytes. To support it, CD14-positive monocytes that were isolated from PBMC promoted IDO1 expression by r-LVRN stimulation. This also demonstrates that r-LVRN can induce IDO1 expression in monocytes without the intervention of other immune cell populations, supporting the direct effects of LVRN on CD14-positive monocyte-lineage cells. PMA treatment was reported to induce macrophage differentiation in THP-1 cells [26]. This study showed that - activated THP-1 cells became more responsive to r-LVRN stimulation and promoted IDO1 expression, suggesting that macrophages increase the reactivity to LVRN in the process of differentiation from monocytes.

The present study also showed that r-LVRN decreased tryptophan level and increased the kynurenine/tryptophan ratio in the culture media of the -treated THP-1 cells, suggesting that the local concentration of tryptophan is regulated by EVT. During the remodeling process of maternal arteries, EVT acquires maternal-fetal immune tolerance from maternal immune cells [5,27,28]. Similar to HLA-G, LVRN is specifically expressed in EVT. Until the end of pregnancy, LVRN-positive EVT abundantly resides around the maternal-fetal interface of the placenta and fetal membrane [14,16]. Consequently, our results suggest that EVT sustainably contributes to creating the local immunosuppressive environment at the maternal-fetal interface throughout the uterus by the action of LVRN.

In conclusion, we first demonstrated that LVRN is involved in IDO1 production by immune cells. The target cells for r-LVRN are CD14-positive monocytes and r-LVRN induces IDO1 expression in monocytes without the intervention of other immune cell populations. The treatment induces THP-1 cells to become more responsive to LVRN, suggesting that activated monocytes promote the reactivity to LVRN. The treatment of r-LVRN also increased the kynurenine/tryptophan ratio around the -treated THP-1 cells, which facilitates an immunosuppressive environment. These findings suggest that LVRN is one of the key molecules that mediate the interaction between EVT and monocytes/macrophages and creates an immunosuppressive environment at the maternal-fetal interface in the uterus.

Limitation of the study

The present study has several limitations. The first is the lack of molecular mechanisms such as intercellular signal transduction, by which LVRN induces IDO1 gene expression in monocytes. The experiment using a variety of inhibitors for signal transduction would be effective to elucidate the molecular mechanisms. The second is the lack of information on the receptor for LVRN. The cell surface molecules that are induced on PMA-activated THP-1

may be potential candidates for the receptor for LVRN. The third is the lack of direct findings that LVRN induces immunotolerance in immune cells. The functional analysis of T lymphocytes that are co-cultured with r-LVRN-treated monocytes or THP-1 cells would be necessary to confirm the immune-tolerant effect of LVRN on immune cells. These issues should be clarified in the future.

Acknowledgements

The authors are grateful to Ms. Ai Sato and Ms. Mai Funamoto for their technical assistance and preparation of the manuscript. This work was supported in part by Grants-in-Aid for Scientific Research (nos. 17H04337, 19K22681, 21H04837, 21K16765, and 22K18396).

References

1. Fujiwara, H., Matsumoto, H., Sato, Y., Horie, A., Ono, M., Nakamura, M., Mizumoto, Y., Kagami, K., Fujiwara, T., Hattori, A., et al. (2018). Factors Regulating Human Extravillous Trophoblast Invasion: Chemokine-peptidase and CD9-integrin Systems. Curr Pharm Biotechnol 19, 764-770. 10.2174/1389201019666181029164906.
2. Albrecht, E.D., and Pepe, G.J. (2020). Regulation of Uterine Spiral Artery Remodeling: a Review. Reprod Sci. 10.1007/s43032-020-00212-8.
3. Lash, G.E., Pitman, H., Morgan, H.L., Innes, B.A., Agwu, C.N., and Bulmer, J.N. (2016). Decidual macrophages: key regulators of vascular remodeling in human pregnancy. J Leukoc Biol 100, 315-325. 10.1189/jlb.1A0815-351R.
4. Robson, A., Harris, L.K., Innes, B.A., Lash, G.E., Aljunaidy, M.M., Aplin, J.D., Baker, P.N., Robson, S.C., and Bulmer, J.N. (2012). Uterine natural killer cells initiate spiral artery remodeling in human pregnancy. FASEB J 26, 4876-4885. 10.1096/fj.12-210310.
5. Zhang, X., and Wei, H. (2021). Role of Decidual Natural Killer Cells in Human Pregnancy and Related Pregnancy Complications. Front Immunol 12, 728291. 10.3389/fimmu.2021.728291.
6. Schumacher, A., and Zenclussen, A.C. (2019). Human Chorionic Gonadotropin-Mediated Immune Responses That Facilitate Embryo Implantation and Placentation. Front Immunol 10, 2896. 10.3389/fimmu.2019.02896.
7. Fujiwara, H., Ono, M., Sato, Y., Imakawa, K., Iizuka, T., Kagami, K., Fujiwara, T., Horie, A., Tani, H., Hattori, A., et al. (2020). Promoting Roles of Embryonic Signals in Embryo Implantation and Placentation in Cooperation with Endocrine and Immune Systems. Int J Mol Sci 21. 10.3390/ijms21051885.
8. Gridelet, V., Perrier d'Hauterive, S., Polese, B., Foidart, J.M., Nisolle, M., and Geenen, V. (2020). Human Chorionic Gonadotrophin: New Pleiotropic Functions for an "Old" Hormone During Pregnancy. Front Immunol 11, 343. 10.3389/fimmu.2020.00343.
9. Tilburgs, T., Crespo, A.C., van der Zwan, A., Rybalov, B., Raj, T., Stranger, B., Gardner, L., Moffett, A., and Strominger, J.L. (2015). Human HLA-G+ extravillous trophoblasts: Immune-activating cells that interact with decidual leukocytes. Proc Natl Acad Sci U S A 112, 7219-7224. 10.1073/pnas.1507977112.
10. Le Bouteiller, P. (2015). HLA-G in human early pregnancy: control of uterine immune cell activation and likely vascular remodeling. Biomed J 38, 32-38. 10.4103/2319-4170.131376.

11. Rajagopalan, S. (2014). HLA-G-mediated NK cell senescence promotes vascular remodeling: implications for reproduction. Cell Mol Immunol 11, 460-466. 10.1038/cmi.2014.53.
12. Yang, Y., Wang, W., Weng, J., Li, H., Ma, Y., Liu, L., and Ma, W. (2022). Advances in the study of HLA class Ib in maternal-fetal immune tolerance. Front Immunol 13, 976289. 10.3389/fimmu.2022.976289.
13. Nilsson, L.L., and Hviid, T.V.F. (2022). HLA Class Ib-receptor interactions during embryo implantation and early pregnancy. Hum Reprod Update 28, 435-454. 10.1093/humupd/dmac007.
14. Fujiwara, H., Higuchi, T., Yamada, S., Hirano, T., Sato, Y., Nishioka, Y., Yoshioka, S., Tatsumi, K., Ueda, M., Maeda, M., and Fujii, S. (2004). Human extravillous trophoblasts express laeverin, a novel protein that belongs to membrane-bound gluzincin metallopeptidases. Biochem Biophys Res Commun 313, 962-968.
15. Maruyama, M., Hattori, A., Goto, Y., Ueda, M., Maeda, M., Fujiwara, H., and Tsujimoto, M. (2007). Laeverin/aminopeptidase Q, a novel bestatin-sensitive leucine aminopeptidase belonging to the M1 family of aminopeptidases. J Biol Chem 282, 20088-20096. 10.1074/jbc.M702650200.
16. Horie, A., Fujiwara, H., Sato, Y., Suginami, K., Matsumoto, H., Maruyama, M., Konishi, I., and Hattori, A. (2012). Laeverin/aminopeptidase Q induces trophoblast invasion during human early placentation. Hum Reprod 27, 1267-1276. 10.1093/humrep/des068.
17. Tsuchiya, S., Yamabe, M., Yamaguchi, Y., Kobayashi, Y., Konno, T., and Tada, K. (1980). Establishment and characterization of a human acute monocytic leukemia cell line (THP- 1). Int J Cancer 26, 171-176. 10.1002/ijc.2910260208.
18. Straszewski-Chavez, S.L., Abrahams, V.M., Alvero, A.B., Aldo, P.B., Ma, Y., Guller, S., Romero, R., and Mor, G. (2009). The isolation and characterization of a novel telomerase immortalized first trimester trophoblast cell line, Swan 71. Placenta 30, 939-948. 10.1016/j.placenta.2009.08.007.
19. Munn, D.H., and Mellor, A.L. (2013). Indoleamine 2,3 dioxygenase and metabolic control of immune responses. Trends Immunol 34, 137-143. 10.1016/j.it.2012.10.001.
20. Kim, M., and Tomek, P. (2021). Tryptophan: A Rheostat of Cancer Immune Escape Mediated by Immunosuppressive Enzymes IDO1 and TDO. Front Immunol 12, 636081. 10.3389/fimmu.2021.636081.
21. Sedlmayr, P., Blaschitz, A., and Stocker, R. (2014). The role of placental tryptophan catabolism. Front Immunol 5, 230. 10.3389/fimmu.2014.00230.
22. Terness, P., Bauer, T.M., Rose, L., Dufter, C., Watzlik, A., Simon, H., and Opelz, G. (2002). Inhibition of allogeneic T cell proliferation by indoleamine 2,3-dioxygenase-expressing dendritic cells: mediation of suppression by tryptophan metabolites. J Exp Med 196, 447- 457. 10.1084/jem.20020052.
23. Munn, D.H., Sharma, M.D., Baban, B., Harding, H.P., Zhang, Y., Ron, D., and Mellor, A.L. (2005). GCN2 kinase in T cells mediates proliferative arrest and anergy induction in response to indoleamine 2,3-dioxygenase. Immunity 22, 633-642. 10.1016/j.immuni.2005.03.013.
24. Mezrich, J.D., Fechner, J.H., Zhang, X., Johnson, B.P., Burlingham, W.J., and Bradfield, C.A. (2010). An interaction between kynurenine and the aryl hydrocarbon receptor can generate regulatory T cells. J Immunol 185, 3190-3198. 10.4049/jimmunol.0903670.
25. True, H., Blanton, M., Sureshchandra, S., and Messaoudi, I. (2022). Monocytes and macrophages in pregnancy: The good, the bad, and the ugly. Immunol Rev 308, 77-92. 10.1111/imr.13080.

26. Daigneault, M., Preston, J.A., Marriott, H.M., Whyte, M.K., and Dockrell, D.H. (2010). The identification of markers of macrophage differentiation in PMA-stimulated THP-1 cells and monocyte-derived macrophages. PLoS One 5, e8668. 10.1371/journal.pone.0008668.
27. Granot, I., Gnainsky, Y., and Dekel, N. (2012). Endometrial inflammation and effect on implantation improvement and pregnancy outcome. Reproduction 144, 661-668. 10.1530/REP-12-0217.
28. Papuchova, H., Meissner, T.B., Li, Q., Strominger, J.L., and Tilburgs, T. (2019). The Dual Role of HLA-C in Tolerance and Immunity at the Maternal-Fetal Interface. Front Immunol 10, 2730. 10.3389/fimmu.2019.02730.
29. Maruyama, M., Arisaka, N., Goto, Y., Ohsawa, Y., Inoue, H., Fujiwara, H., Hattori, A., and Tsujimoto, M. (2009). Histidine 379 of human laeverin/aminopeptidase Q, a nonconserved residue within the exopeptidase motif, defines its distinctive enzymatic properties. J Biol Chem 284, 34692-34702. 10.1074/jbc.M109.066712.
30. Team, R.C. (2023). R: A Language and Environment for Statistical Computing.
31. Matsumoto, T., Iizuka, T., Nakamura, M., Suzuki, T., Yamamoto, M., Ono, M., Kagami, K., Kasama, H., Wakae, K., Muramatsu, M., et al. (2022). FOXP4 inhibits squamous differentiation of atypical cells in cervical intraepithelial neoplasia via an ELF3-dependent pathway. Cancer Sci 113, 3376-3389. 10.1111/cas.15489.
32. Matsumoto, T., Iizuka, T., Nakamura, M., Suzuki, T., Yamamoto, M., Ono, M., Kagami, K., Kasama, H., Wakae, K., Muramatsu, M., et al. (2022). FOXP4 inhibits squamous differentiation of atypical cells in cervical intraepithelial neoplasia via an ELF3-dependent pathway. Cancer Sci. 10.1111/cas.15489.
33. Dochi, H., Kondo, S., Murata, T., Fukuyo, M., Nanbo, A., Wakae, K., Jiang, W.P., Hamabe-Horiike, T., Tanaka, M., Nishiuchi, T., et al. (2022). Estrogen induces the expression of EBV lytic protein ZEBRA, a marker of poor prognosis in nasopharyngeal carcinoma. Cancer Sci 113, 2862-2877. 10.1111/cas.15440.

Figures and Tables

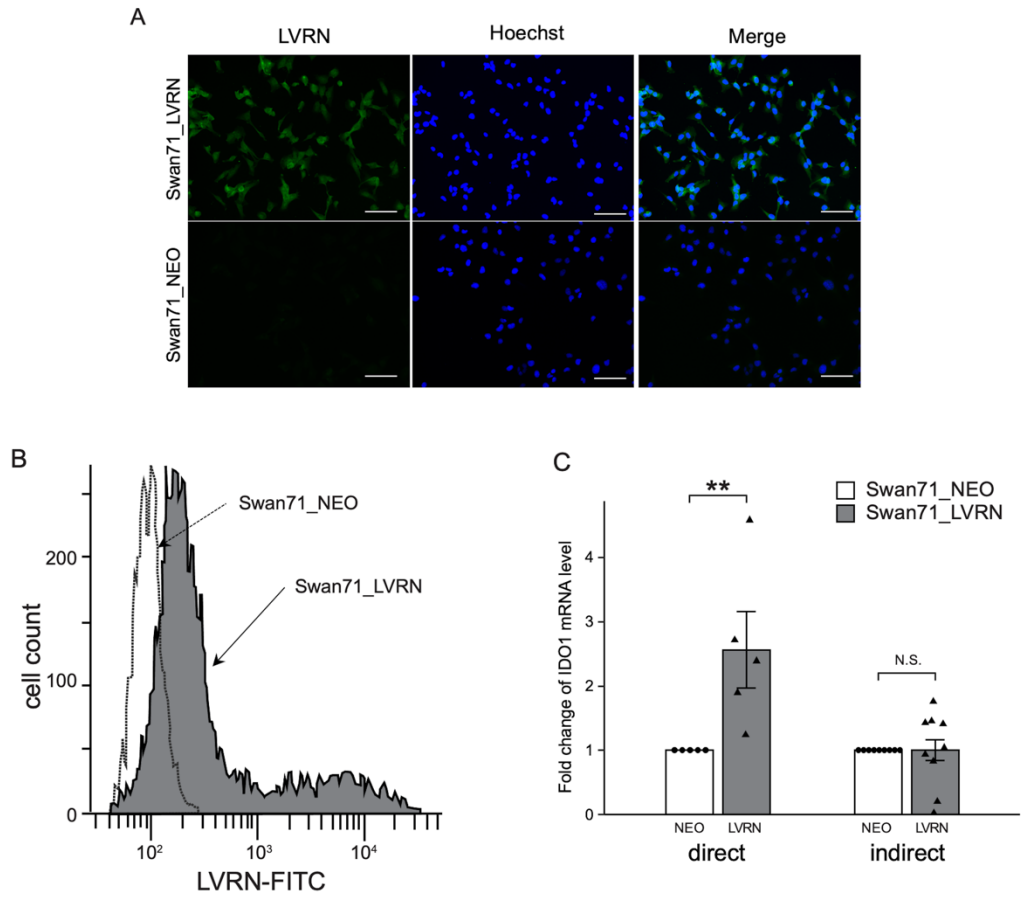

Figure 1. LVRN-transfected Swan71 cells promoted IDO1 expression in PBMC

A: Representative images of immunocytochemistry staining for LVRN (green) in LVRN-transfected Swan71 cells (Swan71_LVRN) and mock-transfected Swan71 cells (Swan71_NEO). Hoechst was used for nuclear staining (blue). Scale bars: 50 μm.

B: Representative histograms of LVRN protein expression in Swan71_LVRN cells and Swan71_NEO cells (dashed line) analyzed by flow cytometry.

C: The bar graph shows the quantification of IDO1 mRNA expression levels in PBMCs by RT-qPCR. Cells were co-cultured with LVRN-transfected and mock-transfected Swan71 cells under direct (n = 5) and indirect conditions (n = 9). Values are presented as mean ± SEM. Statistical analysis was performed using the Wilcoxon signed-rank test. ** $p < 0.01$.

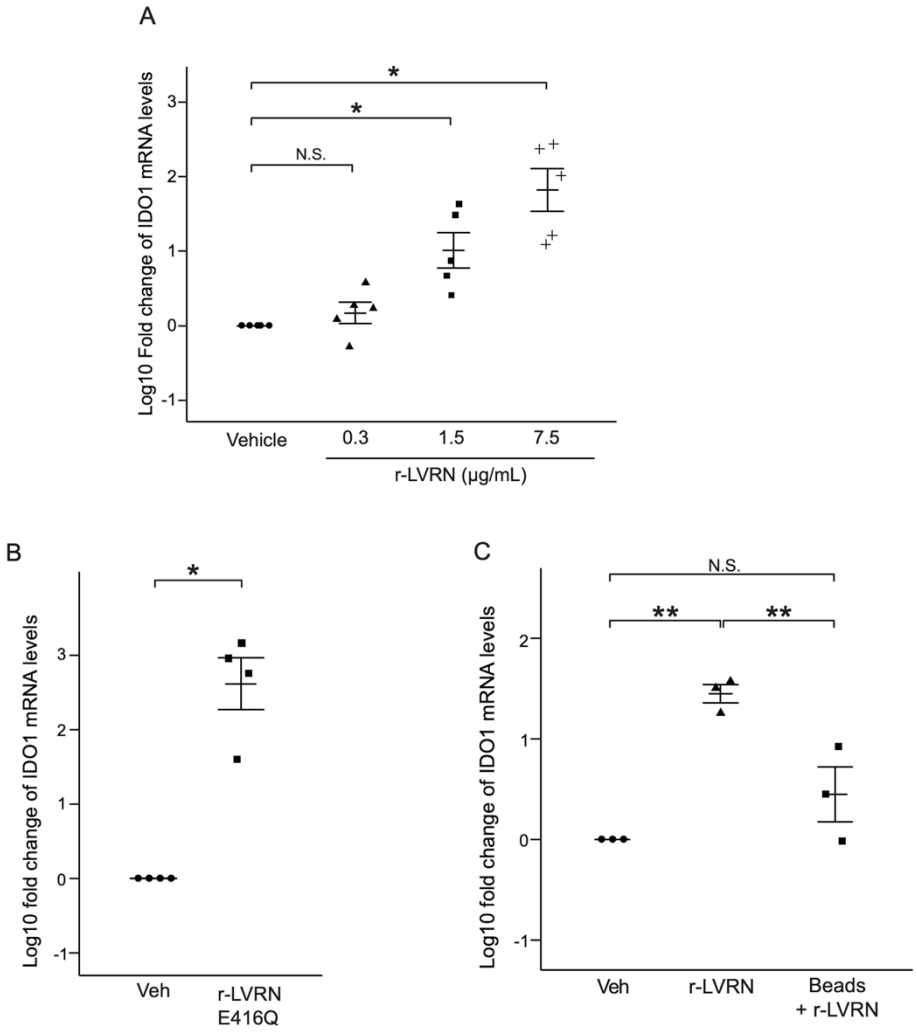

Figure 2. Soluble LVRN promoted IDO1 expression in PBMC

A: The dot plot shows RT-qPCR quantification of IDO1 mRNA expression levels in PBMCs treated with vehicle (PBS) or various concentrations of r-LVRN (0.1, 0.5, and 1.5 μg/mL) for 24 h. Values are presented as mean ± SEM (n = 5). Statistical analysis was performed using the Kruskal-Wallis test with post hoc Wilcoxon signed-rank test with Bonferroni correction for multiple testing. * $p < 0.05$.

B: The dot plot shows RT-qPCR quantification of IDO1 mRNA expression levels in PBMCs treated with vehicle or E416Q mutated r-LVRN (1.5 μg/mL) for 24 h. Values are presented as mean ± SEM (n = 4). Statistical analysis was performed using the Wilcoxon signed-rank test. * $p < 0.05$.

C: The dot plot shows RT-qPCR quantification of IDO1 mRNA expression levels in PBMCs treated with vehicle, r-LVRN (1.5 μg/mL), and solvent after removal of r-LVRN by anti-His-tag antibody-conjugated magnetic beads. Values are presented as mean ± SEM (n = 3). Statistical analysis was performed using One-way ANOVA (Analysis of variance) with post hoc Tukey HSD tests. ** $p < 0.01$.

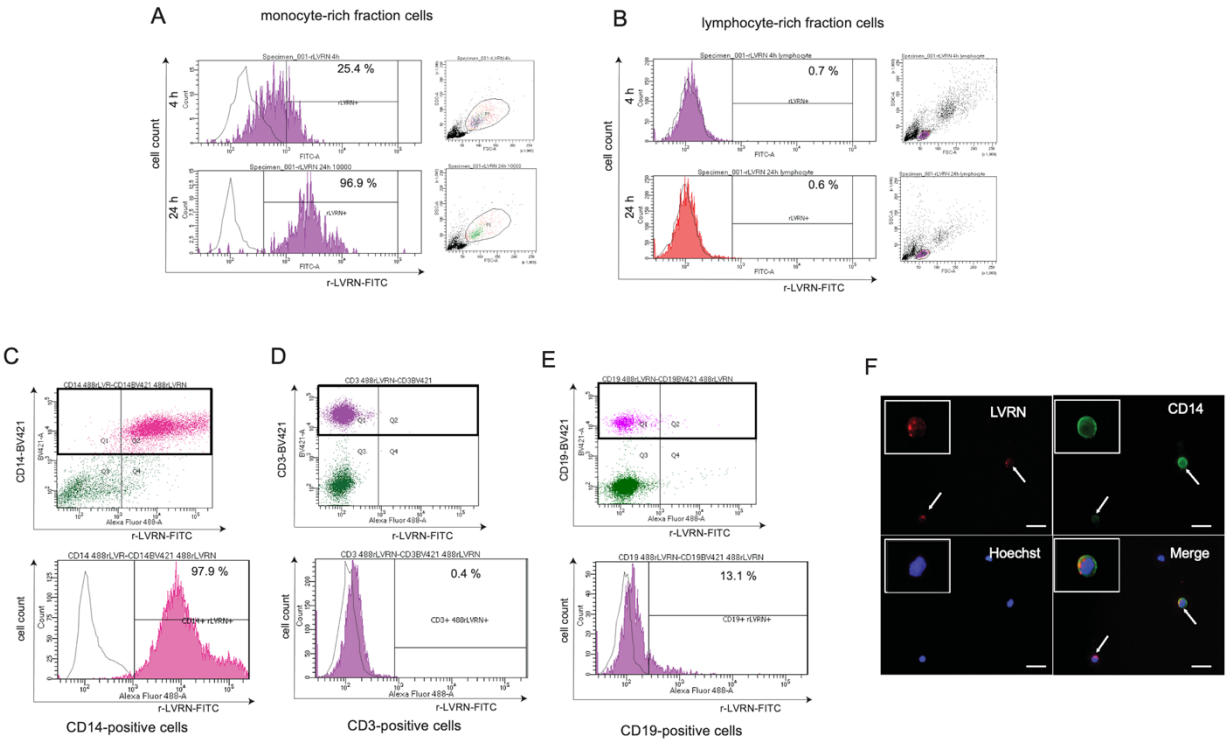

Figure 3. r-LVRN interacted with CD14-positive monocytes

A and B: Representative histograms of r-LVRN-FITC bound monocyte-rich fraction (A) and lymphocyte-rich fraction PBMCs (B) analyzed by flow cytometry. Cells were treated with vehicle (dashed line) or r-LVRN-FITC for 4 h and 24 h.

C to E: Representative histograms of r-LVRN-FITC bound CD14-positive cells (C), CD3-positive cells (D), and CD19-positive cells (E) analyzed by flow cytometry. PBMCs were treated with vehicle (dashed line) or r-LVRN-FITC for 24 h.

F: Representative images of immunocytochemistry staining for CD14 (green, arrows) of r-LVRN- Hylight555 (red) bound PBMCs. Hoechst was used for nuclear staining (blue). The high- magnification images are presented in the upper left corner, respectively. Scale bars: 20 μm.

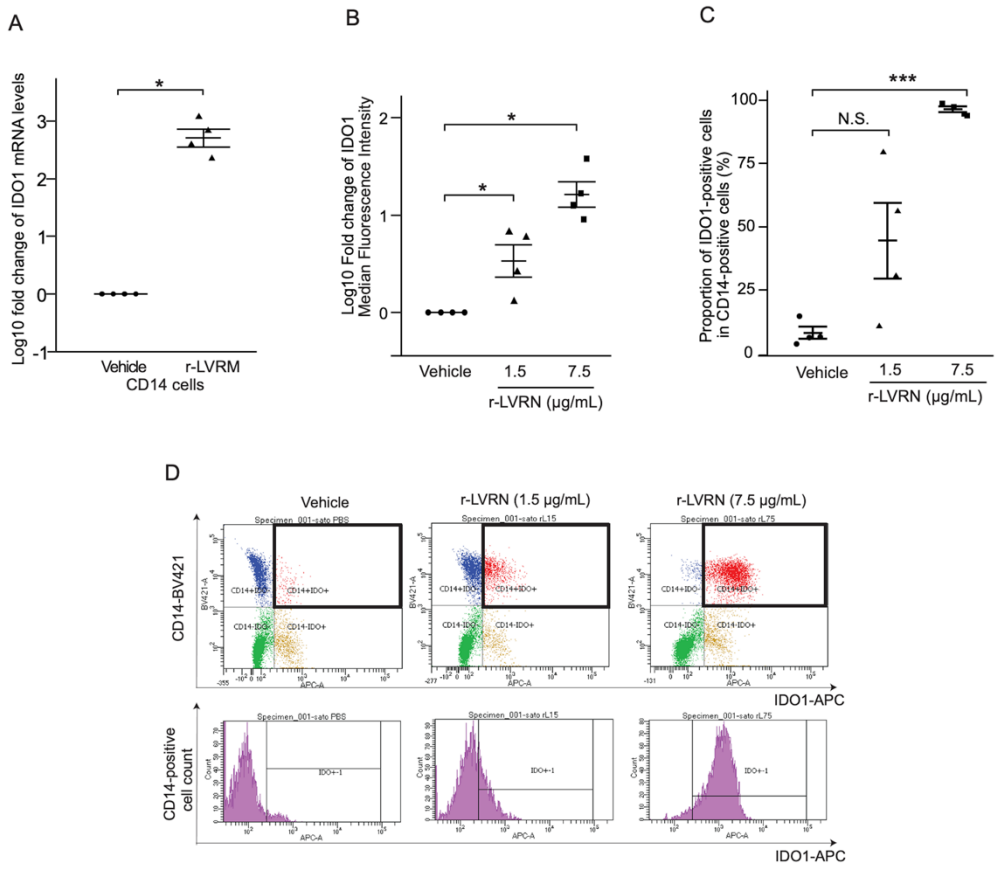

Figure 4. r-LVRN induced IDO1 expression in CD14-positive monocytes

A: The dot plot shows RT-qPCR quantification of IDO1 mRNA expression levels in CD14-positive PBMCs treated with vehicle or r-LVRN (1.5 μg/mL) for 24 h. Values are presented as mean ± SEM (n = 4). Statistical analysis was performed using the Wilcoxon signed-rank test. * $p < 0.05$.

B to D: PBMCs were treated with vehicle and r-LVRN (1.5 and 7.5 μg/mL) for 24 h and analyzed by flow cytometry. The dot plot shows Mean Fluorescence intensity (MFI) of IDO1 protein (B) and positive rate of IDO1 (C) in CD14-positive cells. Representative histograms of IDO1 protein expression in CD14-positive PBMCs treated with r-LVRN (D). Values are presented as mean ±SEM (n = 4). Statistical analysis was performed using the Kruskal-Wallis test with post hoc Wilcoxon signed-rank test with Bonferroni correction for multiple testing. * $p < 0.05$.

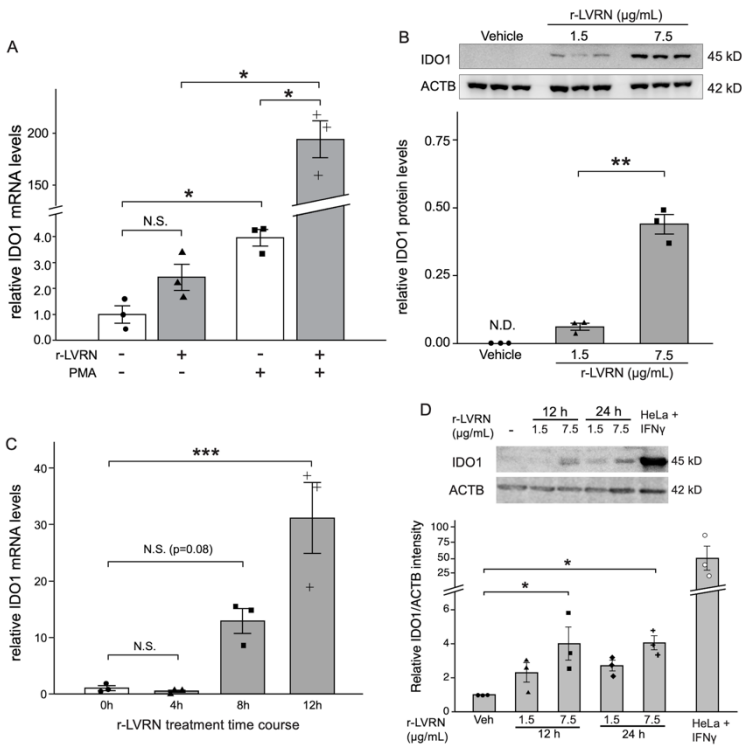

Figure 5. r-LVRN induced IDO1 expression in PMA-stimulated THP-1 cells

A: The bar graph shows RT-qPCR quantification of IDO1 mRNA expression levels in non-activated and activated THP-1 cells treated with vehicle or r-LVRN (1.5 μg/mL) for 24 h. Values are presented as mean ± SEM (n = 3). Statistical analysis was performed using the Welch two- sample t-test with Bonferroni correction for multiple testing. * $p < 0.05$.

B: Representative Immunoblot images showing IDO1 and ACTB protein in activated THP-1 cells treated with vehicle or r-LVRN (1.5 and 7.5 μg/mL) for 48 h. The bar graph shows ImageJ quantification of relative IDO1 protein. IDO1 protein level was normalized to ACTB protein calculating the ratios of the densities of IDO1 and ACTB protein bands. Values are presented as mean ± SEM (n = 3). Statistical analysis was performed using the Welch two-sample t-test. * $p < 0.05$.

C: The bar graph shows RT-qPCR quantification of IDO1 mRNA expression levels in activated THP-1 cells treated with r-LVRN (1.5 μg/mL) for 0, 4, 8, and 12 h. Values are presented as mean± SEM (n = 3). Statistical analysis was performed using One-way ANOVA (Analysis of variance) with post hoc Dennett's multiple comparison test compared with 0 h. *** $p < 0.001$.

D: Representative Immunoblot images showing IDO1 and ACTB protein in activated THP-1 cells treated with vehicle or r-LVRN (1.5 and 7.5 μg/mL) for 12 and 24 h. IDO1 protein in HeLa cells treated with 10 ng/mL of IFNγ for 24 h was shown as a positive control. The ratio of the IDO1 and ACTB protein level was normalized to vehicle control. Values are presented as mean ± SEM (n = 3). Statistical analysis was performed using the Dunnett's multiple comparison test. * $p < 0.05$.

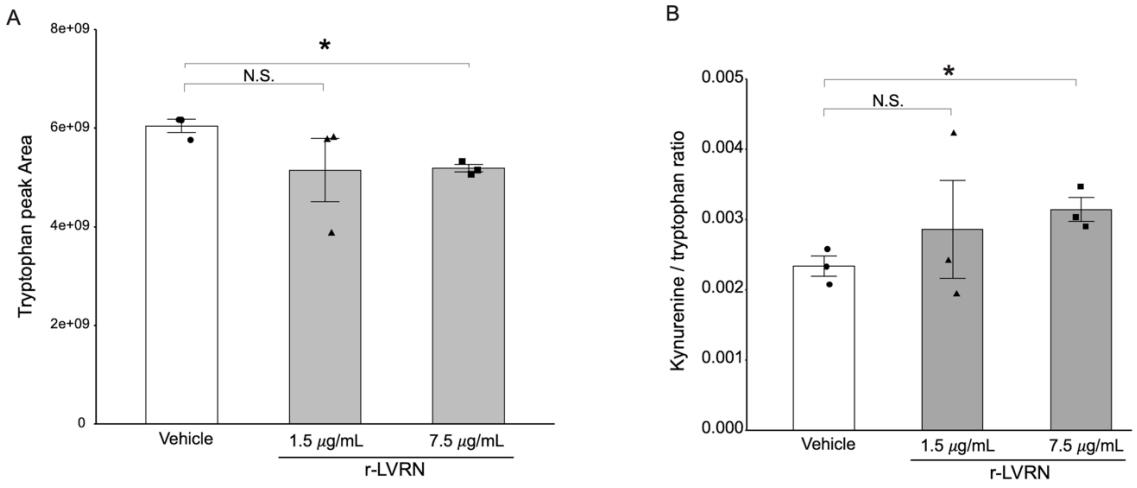

Figure 6. r-LVRN decreased the tryptophan level and increased the kynurenine/ tryptophan ratio in PMA-activated THP-1 cells

A-B: The bar graph shows the tryptophan level (A) and kynurenine/tryptophan ratio (B) in media of activated THP-1 cells treated with vehicle or r-LVRN (1.5 and 7.5 µg/mL) for 48 h. Values are presented as mean ± SEM (n = 3). Statistical analysis was performed using the Welch two-sample test with Bonferroni correction for multiple testing. * $p < 0.05$.

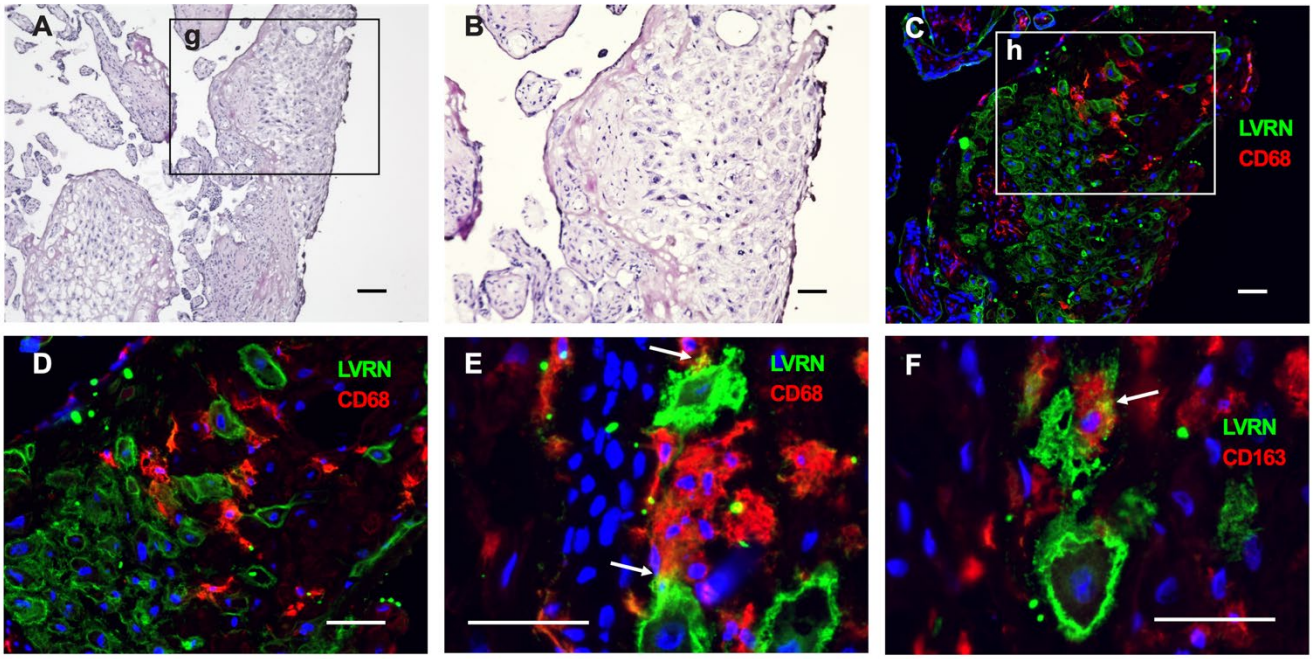

Figure 7. Macrophages are closely associated with LVRN-positive EVT at the maternal-fetal interface of the term placenta

A: Hematoxylin staining of the human term placenta including the maternal-fetal interface of the placental bed (black box). B and C: Magnified images of box g in Figure 7A.

B: Hematoxylin staining. C: Immunofluorescent double staining of LVRN (green) and CD68 (red). Hoechst was used for nuclear staining (blue). D: A magnified image of box h in Figure 7C. CD68-positive macrophages are located around LVRN-positive EVT.

E and F: Magnified images showing the direct interaction (white arrows) between LVRN-positive EVT and CD68-positive macrophages (E) and CD163-positive macrophages (F) in the other sites of the placental bed. Scale bars: A, 100 μm; B-F, 50 μm.